Hue University Journal of Science: Natural Science
Vol. 133, No. 1B, 49–61, 2024

pISSN 1859-1388
eISSN 2615-9678

An Efficient Transmission Power Design for SWIPT Multi-antenna Network Integrated by an Intelligent Reflecting Surface

Pham Viet Tuan*, Hoang Dinh Long, Nguyen Tu Ha, Hoang Trong Duc

Faculty of Physics, University of Education, Hue University, 34 Le Loi, Hue City, Vietnam

* Correspondence to Pham Viet Tuan <pvtuan@hueuni.edu.vn>

(*Received: 20 March 2023; Revised: 27 June 2023; Accepted: 28 October 2023*)

Abstract. In this work, intelligent reflecting surface (IRS) is integrated to improve the transmission power in the simultaneous wireless information and power transfer (SWIPT) system with hybrid time-switching (TS) users. The considered scenario includes one base station (BS), one IRS, and multiple TS users, where the BS transmits the information and energy signals to the receivers with IRS assistance. The sum transmission power minimization problem is formulated under the quality-of-service constraints of data rate and energy harvesting amount at the TS users and the equal time-switching periods. The successive convex approximation and alternating optimization methods are exploited to construct efficient algorithms for finding the suboptimal precoding beamforming vectors at the BS and the phase shifts at the IRS elements. Finally, the numerical results show convergence and significant improvement in performance as compared to conventional baseline schemes.

Keywords: Simultaneous wireless information and power transfer (SWIPT), intelligent reflecting surface (IRS), time-switching (TS) structure, alternating optimization (AO), transmission power minimization

1 Introduction

1.1 Related Works and Motivations

IRS: Recently, Intelligent Reflecting Surfaces (IRSs) have appeared as a favorable technology for sustainable 6G next-generation systems since they are capable of reconfiguring the wireless propagation environment via highly controllable and intelligent signal reflection [1, 2]. Specifically, IRS contains low-cost and passive reflective components, e.g., printed dipoles and phase shifters, each of which can adjust the phase of incoming signals in real time. Thereby, the reflected and direct signals can be incorporated constructively or destructively at receivers. Moreover, the passive components have low-power consumption while reflecting the incident signals without decoding or amplifying them. Furthermore, the IRS arrays are produced in small size and low weight, which allows them to conveniently mount in the building's ceilings, walls, etc. [3-5].

SWIPT: The performances of wireless systems such as cellular networks, wireless sensor networks, wearable wireless network, medical sensor networks, etc. depend on the limited amount of energy in devices' batteries. Therefore, the energy in devices' batteries needs to be recharged or replaced. This requires a high cost, frequent replacement, and much difficulty in some situations, such as wireless sensor networks in construction and the body. The technique of simultaneous wireless information and power transfer (SWIPT) has attracted a lot of attention in both academic and industrial research since it can break the bottleneck of constrained energy in

wireless devices. Wireless power transfer can prolong the lifetime of low-power devices, mobiles, and wireless devices on the Internet of Things without the use of an electric wire for charging [6-8].

In practice, the receivers can separately decode information or harvest energy, or simultaneously receive both information and energy when equipped with the time-switching (TS) or power-splitting (PS) structure. In the PS structure, the incoming signal is divided into two streams, where the first one is used for the ID unit and the other is used for the EH unit according to the power-splitting ratio. In the TS structure, the incoming signal is switched between the information decoding (ID) unit and the energy harvesting (EH) unit according to the time-switching ratio [9, 10].

IRS-aided SWIPT: To exploit the advantages of IRS, the SWIPT networks, integrated with IRS, are expected to enhance the performance of the data and energy efficiencies and compensate for the distance attenuation of RF signals. In [11], the authors investigated the SWIPT network with a single IRS sending both energy and data to two separated groups of energy and information users, where the target is to maximize the harvested energy while guaranteeing the data rate threshold for information users. In previous work of Tang *et al.* [12], they studied the max-min harvested energy of EH users with an energy beamforming vector. The results of harvested energy with IRS are higher than in the conventional SWIPT case without IRS. In addition, the semidefinite relaxation method combined with Gaussian randomization is proposed with high computational complexity. In Ref.[13], with the similar model as Tang, multiple objectives such as harvested energy maximization and sum rate maximization are studied by optimizing the active and passive vectors at the transmitter and IRS. The authors in Ref. [14] studied the SWIPT network with IRS and the hybrid information and energy users with the power-splitting structure. The target is to maximize the minimum individual energy efficiency of the receivers with the non-linear EH model.

In [15], the authors studied energy efficiency maximization (the ratio of the sum rate and consuming energy) while protecting information security from potential eavesdroppers. The model of single multiple-antenna transmitter, two separated groups of information and energy users, one IRS, and the non-linear EH model are considered. In [16], the model of the SWIPT multiple-antenna network with one IRS, one information receiver, multiple energy users, and a group of eavesdroppers is investigated. The target of secrecy rate studied under the harvested energy threshold is limited transmission power is maximized, where the results show the effective IRS exploitation. In [17], the authors studied the SWIPT multiple-antenna network and one IRS where the transmitter sends the energy and information signals to the hybrid users. The problem of energy consumption minimization is solved by jointly optimizing the beamforming vector at the multiple-antenna transmitter, the phase shift at the IRS, and the power-splitting ratios at the hybrid users. In [18], the authors considered the IRS-aided SWIPT network with heterogeneous users and a non-linear EH model. The target of non-linear sum EH energy of multiple types for EH, ID, and hybrid power-splitting users is to maximize with the alternating optimization method.

Besides, in [19], the authors studied the max-min individual information and harvested energy for TS users with the heuristic maximal-ratio transmission (MRT). In [20], Wu *et al.* investigated a novel transmission protocol with

pISSN 1859-1388
eISSN 2615-9678

downlink wireless energy and uplink information transfer for an IRS-aided wireless power communication network. In [21], Zargari *et al.* considered user scheduling and trajectory optimization for the IRS-aided unmanned aerial vehicle (UAV) with SWIPT. However, in the literature, the prior works focused on the scenarios of separated ID and EH users or hybrid power-splitting users, whereas the practical hybrid time-switching users have not been investigated yet. Moreover, the SDR technique generates a high computational solution by shifting the variables from vector to matrix.

1.2 Main Contributions

In the proposed SWIPT network with IRS assistance, the multi-antenna base station transmits data and power to the hybrid TS users for harvesting energy and decoding information. We aim to minimize the sum transmit power at the base station while satisfying the data rate and energy harvesting requirements of the TS users with fixed TS factors. The transmission beamforming vectors at the BS and phase shift vector at the IRS are jointly optimized to reduce power consumption. Our contributions are described as follows**:**

- First, the IRS-integrated SWIPT multi-antenna network with practical time-switching users is proposed**,** and the sum transmission power minimization problem is formulated with joint beamformer and IRS phase shift variables.

- Second, the challenging non-convex sum power optimization problem is solved by the successive convex approximation (SCA) method combined with alternating optimization (AO). The beamforming vectors and the phase shift vector are separated into two subproblems with the second-order cone transformation approach.

- Finally, the numerical experiments evaluate the proposed algorithms and the effectiveness of power gain in the considered IRS-aided SWIPT system in comparison with some baseline schemes.

The rest of this work is structured as follows. The model of the IRS-aided SWIPT network with TS users and the power efficiency problem are shown in Section 2. The proposed solution for the power optimization problem is presented in Section 3. Finally, the numerical experiments are evaluated in Section 4, followed by a conclusion in Section 5.

Notations: Lowercase, boldface lowercase, and boldface uppercase letters are denoted for scalars, vectors, and matrices, respectively. By $\|\mathbf{x}\|$ and $|x|$, we denote the norm-2 of a complex vector $\mathbf{x}$, and the absolute value of a complex scalar x. $\mathrm{diag}\ \mathbf{x}$, represents a diagonal matrix with each diagonal component being the corresponding component in $\mathbf{x}$. We denote $\mathbb{C}^{m\times n}$ for the space of $m\times n$ complex matrices. The identity matrix is denoted by $\mathbf{I}$ with an appropriate size. Lastly, $\mathcal{CN}\ \mathbf{x},\mathbf{\Sigma}$ indicates the distribution of a circularly symmetric complex Gaussian random vector with mean vector $\mathbf{x}$ and covariance matrix $\mathbf{\Sigma}$, where ' ~ 'indicates '*distributed as*'.

2 System Model and Problem Formulation

2.1 System Model

We consider the SWIPT multi-antenna system with the assistance of the IRS and the time-switching users**,** as shown in Fig. 1. The base station (BS) exploits M antennas for transmitting data and energy signals while**,** the users use a single antenna and time-switching architecture. An IRS with N elements reflects the SWIPT transmission signals for supporting the transmission power.

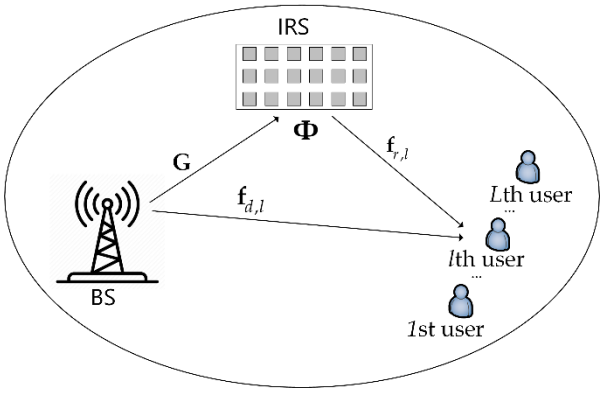

Fig. 1. System model

As seen in Fig. 1, the channels from the BS and IRS to the lth user are $\mathbf{f}_{d,l}, \mathbf{f}_{r,l}$, $\forall l \in \mathcal{L}$ where $\mathbf{f}_{d,l} \in \mathbb{C}^{M\times 1}$, $\mathbf{f}_{r,l} \in \mathbb{C}^{N\times 1}$, and $\mathcal{L} = \{1,2,\cdots,L\}$. Moreover, the BS-IRS channel is denoted as $\mathbf{G} \in \mathbb{C}^{N\times M}$. All incoming signals are reflected by the IRS with the phase shift matrix $\mathbf{\Phi} = \text{diag}\left(e^{j\varphi_1}, e^{j\varphi_2}, \cdots, e^{j\varphi_N}\right)$, where j indicates the imaginary unit and $\varphi_n \in [0, 2\pi)$ represents the reflecting phase adjustment at the nth IRS component, $\forall n \in \mathcal{N} = \{1,2,\cdots,N\}$.

The base station transmits the signal is represented as $\mathbf{x}_B = \sum_{l=1}^{L} \mathbf{b}_l s_l$, where the transmit precoding beamformer $\mathbf{b}_l$ is designed for sending the data symbol s_l to the hybrid lth users. Assuming that the data symbols are the unit power, i.e., $\mathbb{E}\left[s_l s_l^*\right] = 1$ and $\mathbb{E}\left[s_l s_k^*\right] = 0$ $l \neq k$. Therefore, the total transmission power at the BS is calculated as $\mathrm{P}_B = \sum_{l=1}^{L} \left\|\mathbf{b}_l\right\|^2$.

Hence, the reflected IRS signal is given by $\mathbf{x}_{IRS} = \mathbf{\Phi}\mathbf{G}\sum_{l=1}^{L} \mathbf{b}_l s_l$ and the obtained signal at the lth user is expressed as:

$$\begin{aligned} r_l &= \mathbf{f}_{d,l}^H \mathbf{x}_B + \mathbf{f}_{r,l}^H \mathbf{x}_{IRS} + n_l \\ &= \mathbf{f}_{d,l}^H \mathbf{\Phi}\mathbf{G}\sum_{l=1}^{L} \mathbf{b}_l s_l + \mathbf{f}_{r,l}^H \sum_{l=1}^{L} \mathbf{b}_l s_l + n_l \quad , \\ &= \mathbf{f}_{d,l}^H \mathbf{\Phi}\mathbf{G} + \mathbf{f}_{r,l}^H \sum_{l=1}^{L} \mathbf{b}_l s_l + n_l, \forall l \end{aligned} \tag{1}$$

where $n_l \sim \mathcal{CN}\left(0, \sigma_l^2\right)$ is the processing **of** white Gaussian noise (AWGN) at the lth user**,** and the antenna noise is omitted due to its small power.

When the users utilize the TS circuit, the ID operation and the EH operation can be switched for the SWIPT. Without loss of generality, we assume the transmission time of each block is one; thus, the time periods of lth user for the information decoding and the energy harvesting are equal to t_l and $1 - t_l$, respectively. As a result, the harvested power and data rate of the received signal at lth user are expressed as:

$$\Gamma_l = \left(1 - t_l\right) \sum_{k=1}^{L} \left| \mathbf{f}_{d,l}^H + \mathbf{f}_{r,l}^H \mathbf{\Phi}\mathbf{G} \right) \mathbf{b}_k \Big|^2 \tag{2}$$

and

$$\Upsilon_l = t_l \log_2 \left(1 + \frac{\left| \mathbf{f}_{d,l}^H + \mathbf{f}_{r,l}^H \mathbf{\Phi}\mathbf{G} \right) \mathbf{b}_l \Big|^2}{\sum_{k=1, k\neq l}^{L} \left| \mathbf{f}_{d,l}^H + \mathbf{f}_{r,l}^H \mathbf{\Phi}\mathbf{G} \right) \mathbf{b}_k \Big|^2 + \sigma_l^2}\right) \tag{3}$$

respectively. Besides the beamforming vectors of the BS, the IRS phase shifts in reflecting the IRS matrix also affect the harvested energy and data rate at the users**,** as seen in (2) and (3).

2.2 Sum Transmission Power Minimization Problem Formulation

The target of this work is to minimize the sum transmission power under the requirements of energy transfer and data rate in terms of the minimum amount of harvested power and data rate values. In the TS structure, we balance a half time for energy harvesting and a half time for information decoding, i.e., $t_l = 0.5, \forall l$. Thus, the

pISSN 1859-1388
eISSN 2615-9678

transmit beamformers at the BS and the phase shifts at the IRS are optimized in the transmission power minimization problem formulated as follows:

$$(\mathbf{P1}): \underset{\mathbf{b}_l, \varphi_n}{\text{minimize}} \sum_{l=1}^{L} \left\| \mathbf{b}_l \right\|^2 , \quad (4)$$

subject to:

$$1 - t_l \sum_{k=1}^{L} \left\| \mathbf{f}_{d,l}^H + \mathbf{f}_{r,l}^H \mathbf{\Phi} \mathbf{G} \ \mathbf{b}_k \right\|^2 \geq \beta_l, \forall l , \quad (5)$$

$$t_l \log_2 \left(1 + \frac{\left| \mathbf{f}_{d,l}^H + \mathbf{f}_{r,l}^H \mathbf{\Phi} \mathbf{G} \ \mathbf{b}_l \right|^2}{\sum_{k=1, k \neq l}^{L} \left| \mathbf{f}_{d,l}^H + \mathbf{f}_{r,l}^H \mathbf{\Phi} \mathbf{G} \ \mathbf{b}_k \right|^2 + \sigma_l^2} \right) \geq \gamma_l, \forall l \quad (6)$$

$$\left| \mathbf{\Phi}_{n,n} \right| = 1, \forall n . \quad (7)$$

The objective (4) is to minimize the sum transmission power at the base station with the assistance of the IRS, where the sum transmission power with IRS support is expected to reduce in comparison with that of the conventional No-IRS scheme. In the first constraint (5), the amount of harvested energy at the *l*th user is required to be larger than the threshold, β_l (mW). In the second (6), the data rate received by the *l*th user is required to be greater than the threshold, γ_l (bps/Hz). Lastly, the modulus constraint (7) for the phase shift matrix $\mathbf{\Phi}$ guarantees the existence of a reflecting phase at the *n*th element. We observe that the EH and ID constraints are non-convex, along with the modulus constraint. Moreover, the joint beamforming vectors and the phase shifts also make the optimization problem challenging. Thus, the idea of solution method is to exploit the successive convex approximation (SCA) for non-convex constraints and alternating optimization (AO) for the couple of beamformers and phase shifts. In the following section, we propose an efficient, low-complexity algorithm to solve the optimization problem.

3 Proposed Low-complexity Algorithm for Problem (P1)

In this section, the problem (P1) is transformed into a more amenable one, and two groups of beamforming vectors and the phase shifts can be decoupled. As a result, the AO and SCA algorithms can be combined to analyze the modified problem. For the energy harvesting constraints, we change the form:

$$\begin{aligned} & 1 - t_l \sum_{k=1}^{L} \left\| \mathbf{f}_{d,l}^H + \mathbf{f}_{r,l}^H \mathbf{\Phi} \mathbf{G} \ \mathbf{b}_k \right\|^2 \geq \beta_l \\ \Leftrightarrow \ & 0 \geq \frac{\beta_l}{1 - t_l} - \sum_{k=1}^{L} \left\| \mathbf{f}_{d,l}^H + \mathbf{f}_{r,l}^H \mathbf{\Phi} \mathbf{G} \ \mathbf{b}_k \right\|^2, \forall l \end{aligned} \quad (8)$$

For the data rate constraints, we first transform (6) into:

$$\frac{\left| \mathbf{f}_{d,l}^H + \mathbf{f}_{r,l}^H \mathbf{\Phi} \mathbf{G} \ \mathbf{b}_l \right|^2}{\sum_{k=1, k \neq l}^{L} \left| \mathbf{f}_{d,l}^H + \mathbf{f}_{r,l}^H \mathbf{\Phi} \mathbf{G} \ \mathbf{b}_k \right|^2 + \sigma_l^2} \geq \exp\left(\ln 2 \cdot \frac{\gamma_l}{t_l} \right) - 1 . \quad (9)$$

Then, we introduce the auxiliary variables z_l, and Eq. (9) is equivalent to:

$$\begin{aligned} & \left| \mathbf{f}_{d,l}^H + \mathbf{f}_{r,l}^H \mathbf{\Phi} \mathbf{G} \ \mathbf{b}_l \right|^2 \geq z_l \left(\exp\left(\ln 2 \cdot \frac{\gamma_l}{t_l} \right) - 1 \right) \\ & z_l \geq \sum_{k=1, k \neq l}^{L} \left| \mathbf{f}_{d,l}^H + \mathbf{f}_{r,l}^H \mathbf{\Phi} \mathbf{G} \ \mathbf{b}_k \right|^2 + \sigma_l^2 \\ & z_l \geq 0 \end{aligned} \quad . \quad (10)$$

We reformulate the power transmission minimization problem as follows:

$$(\mathbf{P1\text{-}A}): \underset{\mathbf{b}_l, \varphi_n, z_l}{\text{minimize}} \sum_{l=1}^{L} \left\| \mathbf{b}_l \right\|^2 \quad (11)$$

subject to

$$0 \geq \frac{\beta_l}{1 - t_l} - \sum_{k=1}^{L} \left\| \mathbf{f}_{d,l}^H + \mathbf{f}_{r,l}^H \mathbf{\Phi} \mathbf{G} \ \mathbf{b}_k \right\|^2, \forall l \quad (12)$$

$$\left| \mathbf{f}_{d,l}^H + \mathbf{f}_{r,l}^H \mathbf{\Phi} \mathbf{G} \ \mathbf{b}_l \right|^2 \geq z_l \left(\exp\left(\ln 2 \cdot \frac{\gamma_l}{t_l} \right) - 1 \right), \forall l \quad (13)$$

$$z_l \geq \sum_{k=1, k \neq l}^{L} \left| \mathbf{f}_{d,l}^H + \mathbf{f}_{r,l}^H \mathbf{\Phi} \mathbf{G} \ \mathbf{b}_k \right|^2 + \sigma_l^2, \forall l \quad (14)$$

$$z_l \geq 0, \forall l \tag{15}$$

$$\left|\mathbf{\Phi}_{n,n}\right| = 1, \forall n. \tag{16}$$

Then, we alternate to optimize two groups of beamforming vectors and phase shifts in the next subsection.

3.1 Optimizing $\mathbf{b}_l, z_l$ with the given φ_n

We exploit the Taylor expansion for fixed $\mathbf{b}_k^{\,i}, z_l^{\,i}$, thus obtaining the inequality as

$$\left| \mathbf{f}_{d,l}^H + \mathbf{f}_{r,l}^H \mathbf{\Phi G}\ \mathbf{b}_k \right|^2 = \mathbf{b}_k^H \mathbf{f}_l \mathbf{f}_l^H \mathbf{b}_k \geq 2\,\mathrm{Re}\ \mathbf{b}_k^{\,i\,H} \mathbf{f}_l \mathbf{f}_l^H \mathbf{b}_k - \mathbf{b}_k^{\,i\,H} \mathbf{f}_l \mathbf{f}_l^H \mathbf{b}_k^{\,i}, \forall k,l \tag{17}$$

with $\mathbf{f}_l^H = \mathbf{f}_{d,l}^H + \mathbf{f}_{r,l}^H \mathbf{\Phi G}, \forall l$. We introduce the slack variables $p_{1,l}, p_{2,l}, p_{3,l}$ to achieve feasible initial points for the SCA algorithm. At the fixed point $\mathbf{b}_k^{\,i}, z_l^{\,i}$, we derive the convex approximation subproblem [22] as follows:

$$(\mathbf{P2}): \underset{\mathbf{b}_l, z_l, p_{1,l}, p_{2,l}, p_{3,l}}{\text{minimize}} \sum_{l=1}^{L} \left\|\mathbf{b}_l\right\|^2 + \lambda_1 \sum_{l=1}^{L} p_{1,l} + p_{2,l} + p_{3,l} \tag{18}$$

subject to

$$0 \geq -\sum_{k=1}^{L} 2\,\mathrm{Re}\ \mathbf{b}_k^{\,i\,H} \mathbf{f}_l \mathbf{f}_l^H \mathbf{b}_k - \mathbf{b}_k^{\,i\,H} \mathbf{f}_l \mathbf{f}_l^H \mathbf{b}_k^{\,i} + \frac{\beta_l}{1-t_l} - p_{1,l}, \forall l \tag{19}$$

$$0 \geq z_l \left(\exp\left(\ln 2 \cdot \frac{\gamma_l}{t_l} \right) - 1 \right) - 2\,\mathrm{Re}\ \mathbf{b}_l^{\,i\,H} \mathbf{f}_l \mathbf{f}_l^H \mathbf{b}_l - \mathbf{b}_l^{\,i\,H} \mathbf{f}_l \mathbf{f}_l^H \mathbf{b}_l^{\,i} - p_{2,l}, \forall l \tag{20}$$

$$0 \geq \sum_{k=1,k\neq l}^{L} \left| \mathbf{f}_{d,l}^H + \mathbf{f}_{r,l}^H \mathbf{\Phi G}\ \mathbf{b}_k \right|^2 + \sigma_l^2 - z_l - p_{3,l}, \forall l \tag{21}$$

$$z_l \geq 0, p_{1,l} \geq 0, p_{2,l} \geq 0, p_{3,l} \geq 0, \forall l. \tag{22}$$

Then, we exploit MATLAB's CVX tool [23] to achieve the optimal beamforming vectors in the *i*th subproblem. By inserting the new variables $p_{1,l}, p_{2,l}, p_{3,l}$, we are able to start at any initial point, such as $\mathbf{b}_l^{\,0} = [1,\ldots,1]^T$ and $z_l^{\,0} = 1$. As a result, the proposed iterative algorithm is described in Table 1.

Table 1. Algorithm 1 for obtaining the BS beamformers

1	**initialization:**
2	Start a feasible initial point of problem (P1-A). Set $i = 0$.
3	**repeat**
4	Solve the problem (P1-A) to obtain $\mathbf{b}_l, z_l, p_{1,l}, p_{2,l}, p_{3,l}$ with a fixed point $\mathbf{b}_l^{\,i}, z_l^{\,i}$.
5	Update $\mathbf{b}_l^{\,i+1} = \mathbf{b}_l$.
6	Set $i = i+1$
7	**until** satisfying convergent criteria.
8	**output:** Obtained solution $\mathbf{b}_l^{\,i}, z_l^{\,i}$, and sum transmission power $\sum_{l=1}^{L} \left\|\mathbf{b}_l^{\,i}\right\|^2$.

3.2 Optimizing φ_n with the given $\mathbf{b}_l, z_l$

In the following, we find the phase shifts $\{\varphi_n\}$ with the obtained $\mathbf{b}_l, z_l$ by Algorithm 1 in Table 1. Then, we derive the problem from (P1-A):

(**P3**): Find $\mathbf{\Phi}$ subject to

$$0 \geq \frac{\beta_l}{1-t_l} - \sum_{k=1}^{L} \left| \mathbf{f}_{d,l}^H + \mathbf{f}_{r,l}^H \mathbf{\Phi G}\ \mathbf{b}_k \right|^2, \forall l \tag{23}$$

pISSN 1859-1388
eISSN 2615-9678

$$0 \geq z_l\left(\exp\left(\ln 2 \cdot \frac{\gamma_l}{t_l}\right)-1\right) - \left|\mathbf{f}_{d,l}^H + \mathbf{f}_{r,l}^H \mathbf{\Phi G}\ \mathbf{b}_l\right|^2, \forall l \quad (24)$$

$$0 \geq \sum_{k=1,k\neq l}^{L}\left|\mathbf{f}_{d,l}^H + \mathbf{f}_{r,l}^H \mathbf{\Phi G}\ \mathbf{b}_k\right|^2 + \sigma_l^2 - z_l, \forall l \quad (25)$$

$$\left|\mathbf{\Phi}_{n,n}\right| = 1, \forall n. \quad (26)$$

We denote $\mathbf{a} = \left[e^{-j\varphi_1}, e^{-j\varphi_2}, ..., e^{-j\varphi_N}\right]^T$, then derive as

$$\left|\mathbf{f}_{d,l}^H + \mathbf{f}_{r,l}^H \mathbf{\Phi G}\ \mathbf{b}_k\right|^2 = \left|\mathbf{f}_{d,l}^H + \mathbf{a}^H diag\ \mathbf{f}_{r,l}^H\ \mathbf{G}\ \mathbf{b}_k\right|^2 = \left|\mathbf{f}_{d,l}^H \mathbf{b}_k + \mathbf{a}^H diag\ \mathbf{f}_{r,l}^H\ \mathbf{G}\mathbf{b}_k\right|^2 = \left|c_{l,k} + \mathbf{a}^H d_{l,k}\right|^2 \quad (27)$$

where $c_{l,k} = \mathbf{f}_{d,l}^H \mathbf{b}_k$ and $d_{l,k} = diag\ \mathbf{f}_{r,l}^H\ \mathbf{G}\mathbf{b}_k$. Then,

$$\left|c_{l,k} + \mathbf{a}^H \mathbf{d}_{l,k}\right|^2 = \left(c_{l,k} + \mathbf{a}^H \mathbf{d}_{l,k}\right)^H \left(c_{l,k} + \mathbf{a}^H \mathbf{d}_{l,k}\right) = c_{l,k}^H c_{l,k} + 2\,\mathrm{Re}\left(c_{l,k}^H \mathbf{d}_{l,k}\right)^H \mathbf{a} + \mathbf{a}^H \mathbf{d}_{l,k} \mathbf{d}_{l,k}^H \mathbf{a} \quad (28)$$

We use Eq. (28) to obtain the expressions as

$$\sum_{k=1}^{L}\left|\mathbf{f}_{d,l}^H + \mathbf{f}_{r,l}^H \mathbf{\Phi G}\ \mathbf{b}_k\right|^2 = \sum_{k=1}^{L} c_{l,k}^H c_{l,k} + 2\,\mathrm{Re}\left\{\left(\sum_{k=1}^{L} c_{l,k}^H \mathbf{d}_{l,k}\right)^H \mathbf{a}\right\} + \mathbf{a}^H\left(\sum_{k=1}^{L} \mathbf{d}_{l,k}\mathbf{d}_{l,k}^H\right)\mathbf{a} \quad (29)$$

$$\sum_{k=1,k\neq l}^{L}\left|\mathbf{f}_{d,l}^H + \mathbf{f}_{r,l}^H \mathbf{\Phi G}\ \mathbf{b}_k\right|^2 = \sum_{k=1,k\neq l}^{L} c_{l,k}^H c_{l,k} + 2\,\mathrm{Re}\left\{\left(\sum_{k=1,k\neq l}^{L} c_{l,k}^H \mathbf{d}_{l,k}\right)^H \mathbf{a}\right\} + \mathbf{a}^H\left(\sum_{k=1,k\neq l}^{L} \mathbf{d}_{l,k}\mathbf{d}_{l,k}^H\right)\mathbf{a} \quad (30)$$

And we use the following approximations as

$$\mathbf{a}^H\left(\sum_{k=1}^{L} \mathbf{d}_{l,k}\mathbf{d}_{l,k}^H\right)\mathbf{a} \geq 2\,\mathrm{Re}\left\{\mathbf{a}^{i'H}\left(\sum_{k=1}^{L} \mathbf{d}_{l,k}\mathbf{d}_{l,k}^H\right)\mathbf{a}\right\} - \mathbf{a}^{i'H}\left(\sum_{k=1}^{L} \mathbf{d}_{l,k}\mathbf{d}_{l,k}^H\right)\mathbf{a}^{i'}, \quad (31)$$

$$\mathbf{a}^H \mathbf{d}_{l,l}\mathbf{d}_{l,l}^H \mathbf{a} \geq 2\,\mathrm{Re}\ \mathbf{a}^{i'H}\mathbf{d}_{l,l}\mathbf{d}_{l,l}^H\mathbf{a} - \mathbf{a}^{i'H}\mathbf{d}_{l,l}\mathbf{d}_{l,l}^H\mathbf{a}^{i'}. \quad (32)$$

For the constraint $\left|\mathbf{\Phi}_{n,n}\right| = 1, \forall n$, i.e., $\left|a_n\right|^2 = 1, \forall n$, that is equivalent to $0 \geq 1 - \left|a_n\right|^2, \forall n$ and $0 \geq \left|a_n\right|^2 - 1, \forall n$, where the equality is converted to two inequalities. Then, we approximate the non-convex constraint as

$$\left|a_n\right|^2 \geq 2\,\mathrm{Re}\ a_n^{i'*} a_n - \left|a_n^{i'*}\right|^2, \forall n. \quad (33)$$

To start at a feasible point, we introduce the auxiliary variables $\alpha_{1,l}, \alpha_{2,l}, q_{1,n}, q_{2,n}$ in the inequality constraints. At the fixed point $a_n^{i'}$, we then obtain the convex subproblem as follow (**P3-A**):

$$\underset{\left\{a_n, \alpha_{1,l}, \alpha_{2,l}, q_{1,n}, q_{2,n}\right\}}{\text{minimize}} \left(-\sum_{l=1}^{L} \alpha_{1,l} + \alpha_{2,l} + \lambda_2 \sum_{n=1}^{N} q_{1,n} + q_{2,n}\right) \quad (34)$$

subject to

$$\left(\begin{array}{l} \sum_{k=1}^{L} c_{l,k}^H c_{l,k} + 2\,\mathrm{Re}\left\{\left(\sum_{k=1}^{L} c_{l,k}^H \mathbf{d}_{l,k}\right)^H \mathbf{a}\right\} \\ +2\,\mathrm{Re}\left\{\mathbf{a}^{i'H}\left(\sum_{k=1}^{L} \mathbf{d}_{l,k}\mathbf{d}_{l,k}^H\right)\mathbf{a}\right\} \\ -\mathbf{a}^{i'H}\left(\sum_{k=1}^{L} \mathbf{d}_{l,k}\mathbf{d}_{l,k}^H\right)\mathbf{a}^{i'} \end{array}\right) \geq \frac{\beta_l}{\left(-t_l\right)} + \alpha_{1,l}, \forall l \quad (35)$$

$$\left(\begin{array}{l} c_{l,k}^H c_{l,k} + 2\,\mathrm{Re}\left(c_{l,k}^H \mathbf{d}_{l,k}\right)^H \mathbf{a} + \\ 2\,\mathrm{Re}\ \mathbf{a}^{i'H}\mathbf{d}_{l,l}\mathbf{d}_{l,l}^H\mathbf{a} - \mathbf{a}^{i'H}\mathbf{d}_{l,l}\mathbf{d}_{l,l}^H\mathbf{a}^{i'} \end{array}\right) \geq z_l\left(\exp\left(\ln 2 \cdot \frac{\gamma_l}{t_l}\right)-1\right) + \alpha_{2,l}, \forall l \quad (36)$$

$$0 \geq \sum_{k=1,k\neq l}^{L} c_{l,k}^H c_{l,k} + 2\,\mathrm{Re}\left\{\left(\sum_{k=1,k\neq l}^{L} c_{l,k}^H \mathbf{d}_{l,k}\right)^H \mathbf{a}\right\} + \mathbf{a}^H\left(\sum_{k=1,k\neq l}^{L} \mathbf{d}_{l,k}\mathbf{d}_{l,k}^H\right)\mathbf{a} + \sigma_l^2 - z_l, \forall l \quad (37)$$

$$0 \geq \left|a_n\right|^2 - 1 - q_{1,n}, \forall n \tag{38}$$

$$0 \geq 1 - \left(2\,\mathrm{Re}\ \ a_n^{i'*} a_n \ - \left|a_n^{i'*}\right|^2\right) - q_{2,n}, \forall n \tag{39}$$

$$\alpha_{1,l} \geq 0, \alpha_{2,l} \geq 0, q_{1,n} \geq 0, q_{1,n} \geq 0, \forall l, n\,. \tag{40}$$

Then, the fixed point $a_n^{i'}$ is updated by the optimal solution of Problem (P3-A) until convergence.

Table 2. Algorithm 2 for obtaining IRS phase shifts

initialization:
Start an initial point of (P3-A) as a_n^0 . Set $i' = 0$.
repeat
Solve problem (P3-A) via CVX to obtain the optimal solution $a_n, \alpha_{1,l}, \alpha_{2,l}, q_{1,n}, q_{2,n}$ with a fixed point $a_n^{i'}$.
Assign $a_n^{i'+1} = a_n$.
Set $i' = i' + 1$.
until obtaining convergent conditions.
output: Obtained solution $a_n^{i'}$, and shift-phase $\varphi_n = -\mathrm{angle}\ a_n^{i'}$, $\forall n$.

3.3 Overall AO Algorithm

Finally, we present the overall alternating optimization algorithm to achieve the optimal AP beamformer and the IRS shift-phases in Table 3.

Table 3. Algorithm 3 with the overall AO method to solve problem (P1)

1	**initialization:**
2	Start an initial shift-phases φ_n^0 , maximum iteration number, $I_{\max}$.
3	**for** $m = 1$ **to** $I_{\max}$ **do**
4	Update $\mathbf{b}_l^{m+1}, z_l^{m+1}$ by solving problem (P2) with Algorithm 1 in Table 1 when given φ_n^m .
5	**if** satisfying accuracy **then**
6	break;
7	**end if**
8	Update φ_n^{m+1} by solving problem (P3) with Algorithm 2 in Table 2 when given $\mathbf{b}_l^{m+1}, z_l^{m+1}$.
9	**end for**
10	**output:** $\mathbf{b}_l, \varphi_n \leftarrow \mathbf{b}_l^{m+1}, \varphi_n^{m+1}$ and $\sum_{l=1}^{L} \left\|\mathbf{b}_l\right\|^2 \leftarrow \sum_{l=1}^{L} \left\|\mathbf{b}_l^{m+1}\right\|^2$.

The overall AO algorithm is to solve (P1) and (P2) alternatively in an iterative manner with two blocks of variables, $\mathbf{b}_l, z_l$ and φ_n . The local optimal solutions of two blocks are achieved by Algorithm 1 and Algorithm 2, respectively. The computational complexity of Algorithm 1 is $\mathcal{O}\ I_1 L^{3.5} M^3$, where I_1 is the number of iterations in Algorithm 1 and $\mathcal{O}\cdot$ is the big-O notation [24, 25]. The complexity of Algorithm 2 is $\mathcal{O}\ I_2 L N^3$, which I_2 the number of iterations.

pISSN 1859-1388
eISSN 2615-9678

Then, for the overall AO method, the total complexity of Algorithm 3 is $\mathcal{O}\left(I_3\left(I_1L^{3.5}M^3+I_2LN^3\right)\right)$. We note that the proposed method provides low complexity in comparison with the complexity of the semidefinite relaxation (SDR) method with the order of $M^{6.5}$ and $N^{6.5}$ [26].

4 Numerical Results

In this section, the numerical experiments are presented to evaluate the results of the proposed method. The simulated network setup is assumed as follows. The BS is located at (0 m, 0 m), and the IRS is fixed at (3 m, 2 m). Simultaneously, L single-antenna users are uniformly distributed on a circle centered at (5 m, 0 m) with a radius of 0.5 m. The distance-dependent (large-scale) path loss for all channels is expressed as $PL = PL_0 - 10\alpha\log_{10}\left(\frac{d}{d_0}\right)\text{dB}$, where α is the path loss exponent, $PL_0 = -30\,\text{dB}$ is the link distance in meters, and is the path loss at the reference distance of $d_0 = 1\,\text{m}$ [27, 28]. The path loss exponents for the BS-IRS channel, the BS-user channels, and the IRS-user channels are given as $\alpha_{\text{BI}} = 2.2$, $\alpha_{\text{Bu}} = 3.6$, and $\alpha_{\text{Iu}} = 2.2$, respectively [29, 30]. We note that the path loss factor from the base station to the users are large due to the obstacles; thus, the the direct signals to the users with high attenuation is compensated by the indirect reflecting signals with low path loss factors. The Rician model is applied for small-scale fading in every channel where the Rician factor is assigned 3 dB. Moreover, the number of users is $L = 2$ and the antenna noises at the users are $\sigma_l^2 = -90\,\text{dBm}, \forall l$.

4.1 Convergent Behavior

The convergent characteristics of the AO algorithm with $M = 4$ and $N = 5$ are presented in Figure 2. We observe that the values of sum transmission power decrease and achieve convergence under 15 iterations for several random channel examples. Then, the maximum iteration number of the AO algorithm is set at $I_3 = 15$ for convergent assurance in the experiments.

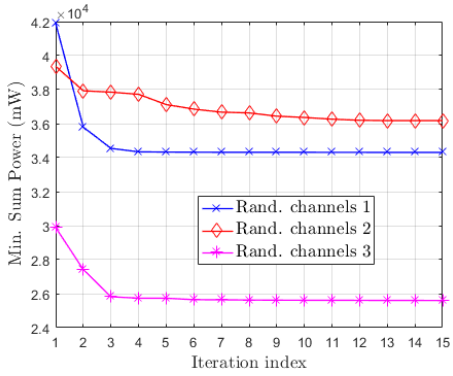

Fig. 2. The convergence behavior of proposed alternating optimization algorithm with several random channels

4.2 Effect of data rate and energy harvesting thresholds

As seen in Fig. 3, the results of sum transmission power are shown versus the required data rate threshold with the number of antennas, $M = 8$, the number of IRS elements, $N = 20$, and the energy harvesting threshold, $\beta_l = -12, -15\,\text{dBm}$.

We also perform two baseline schemes, with the fixed-phase IRS and the No-IRS in comparison to the proposed scheme. In the fixed-phase IRS scheme, the phase shifts at IRS elements are initially assigned, and thus the optimization variables remain the beamforming vectors. In this work, we set the fixed phases as $\varphi_n = \frac{\pi}{3}, \forall n$ for every IRS element in this simple scheme.

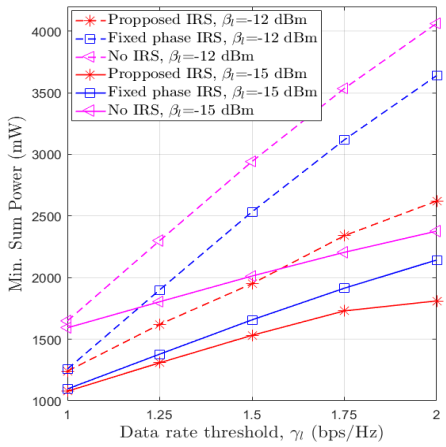

Fig. 3. Min. sum power versus required data rate threshold at TS users

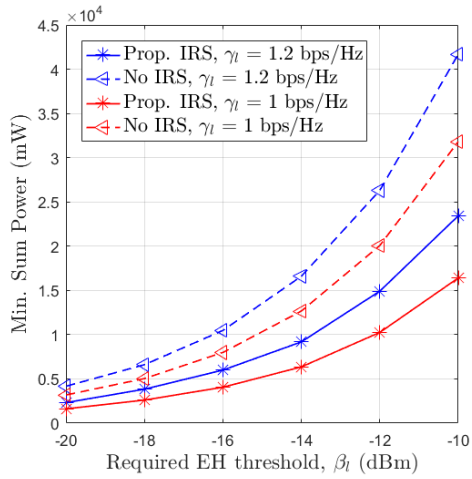

Fig. 4. Min. sum power versus required energy harvesting threshold at TS users

In the second No-IRS baseline scheme, the conventional SWIPT system without IRS is performed. We observe that the proposed method with IRS aid provides lower transmission power than that of the benchmarks. The performance presents the effectiveness of IRS support because the phase shifts are adjusted to improve the desired signals for satisfying the quality of services at the TS users. In addition, the sum transmission power increases with the rise of the data rate thresholds since the base station has to use more power to afford the higher required data rate at the receivers.

In Fig. 4, the impact of the required energy harvesting threshold, β_l, is studied with $M = 4$ and $N = 25$. It can be observed from this plot that the sum transmission powers obtained by all schemes increase along with increasing β_l because the base station needs to consume more power for the high required harvested energy at the users. This figure also expresses that the proposed scheme with carefully optimized phase shifts utilizes better transmission power than the No-IRS baseline scheme does.

Moreover, when the number of users increases, the base station uses more energy to transmit the additive symbols to the new users. Also, the inter-user interference from the new users to the available ones makes the base station increase the transmission power to combat the new interference. Thus, the transmission power of the base station will increase with the rise in the number of users. We observe that the values of the channels in the distance-dependent path loss are affected by the path loss factors and the distances of the base station, the intelligent reflecting surface, and the users. Obviously, when the positions of the users are near the base station and the IRS, we obtain lower values for the sum transmission power due to the lower distance and vice versa.

We observe that the sum power target for $\gamma_l = 1\,\text{bps/Hz}$ is only 1000 mW in Fig. 3, which is better than 10.000 mW in Fig. 4. The reason is that we use more antenna numbers, $M = 8$, and the lower EH threshold $\beta_l = -15\,\text{dBm}$ for Fig. 3, in comparison with antenna numbers, $M = 4$, and the EH threshold $\beta_l = -12\,\text{dBm}$ for Fig. 4.

pISSN 1859-1388
eISSN 2615-9678

4.3 Effect of number IRS elements

We present the impact of the IRS element number on the performance of the proposed and fixed phased schemes in Fig. 5 with $M = 10$, $\beta_l = -10\,\text{dBm}$, and $\gamma_l = 1\,\text{bps/Hz}$. As expected, the sum transmission powers significantly decrease with the increase in IRS element number, N, since a greater degree of freedom availability is used for optimizing the system results. Furthermore, as shown in Fig. 5, the considered system with IRS support consumes less energy than the fixed-phase IRS scheme. The performance illustrates that integrating IRS into the TS-SWIPT network is a promising approach to saving communication energy.

Since the harvested power and data rate of the received power in the conditions (5) and (6) have to be larger than the required thresholds, the total transmission power has a lower bound when the IRS number becomes very large. In the case of a single user in the conventional IRS-aided system, when the IRS element number becomes large, the transmission power of the BS can scale down by a factor of $\frac{1}{N^2}$ as in [31, 32]. However, this is only used for the far-field approximation of IRS elements, as detailed in the analysis in [32].

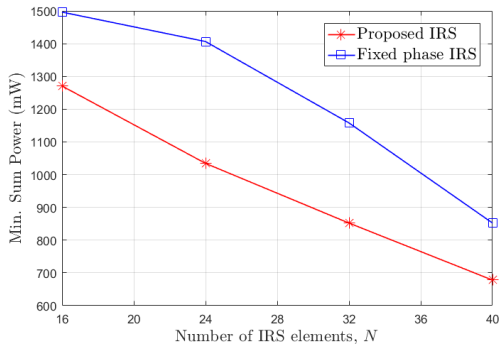

Fig. 5. Min. sum power versus IRS element number

5 Conclusion

In this work, the sum transmission power was minimized in the considered TS-SWIPT multi-antenna system with the assistance of an IRS. The low-complexity algorithm design with the SCA and AO techniques was formulated to optimize the beamforming vectors at the BS and the phase shift vector at the IRS. The simulation investigations unveiled the effectiveness of the IRS in reducing the power consumption of the considered scheme in comparison with the benchmark cases. The discrete phase shifts at the IRS and the impact of the imperfect channel in estimation are open issues for future research. In addition, we need to investigate the position for the IRS to achieve lower sum power with fixed positions for the BS and the users. A study of the asymptotic behavior of large N with near-field approximation is also a challenging issue. These ideas are interesting research directions for our future work.

Acknowledgement

This work was funded by Hue University under grant No. DHH2022-03-169. This work was partially supported by Hue University under the Core Research Program, Grant No. NCM.DHH.2022.08.

References

1. Di Renzo M, Zappone A, Debbah M, Alouini MS, Yuen C, De Rosny J, et al. Smart radio environments empowered by reconfigurable intelligent surfaces: How it works, state of research, and road ahead. IEEE J Sel Areas Commun. 2020;38(11):2450-2525.
2. Wu Q , Zhang R. Towards smart and reconfigurable environment: Intelligent reflecting surface aided wireless network. IEEE communications magazine. 2019;58(1):106-12.
3. Gong S, Lu X, Hoang DT, Niyato D, Shu L, Kim DI, et al. Towards smart radio environment for

wireless communications via intelligent reflecting surfaces: A comprehensive survey. IEEE Commun. Surveys Tut. 2020;22(4):2283-2314.

4. Wu Q, Zhang S, Zheng B, You C, Zhang R. Intelligent reflecting surface-aided wireless communications: A tutorial. IEEE Transactions on Communications. 2021;69(5):3313-51.
5. Zheng B, You C, Mei W, Zhang R. A survey on channel estimation and practical passive beamforming design for intelligent reflecting surface aided wireless communications. IEEE Communications Surveys & Tutorials. 2022;24(2):1035-71.
6. Ding Z, Zhong C, Ng DWK, Peng M, Suraweera HA, Schober R, et al. Application of Smart Antenna Technologies in Simultaneous Wireless Information and Power Transfer. IEEE Commun. Magazine. 2015;53(4):86-93.
7. Qi Q, Chen X, Ng DWK. Robust beamforming for NOMA-based cellular massive IoT with SWIPT. IEEE Trans Signal Process. 2020;68(211):211-24.
8. Zhang R, Ho CK. MIMO broadcasting for simultaneous wireless information and power transfer. IEEE Transactions on Wireless Communications. 2013;12(5):1989-2001.
9. Clerckx B, Zhang R, Schober R, Ng DWK, Kim DI, Poor HV. Fundamentals of Wireless Information and Power Transfer: From RF EnergyHarvester Models to Signal and System Designs. IEEE J Sel Areas Commun. 2019;37(1):4-33.
10. Clerckx B, Huang K, Varshney LR, Ulukus S, Alouini MS. Wireless power transfer for future networks: Signal processing, machine learning, computing, and sensing. IEEE Journal of Selected Topics in Signal Processing. 2021;15(5):1060-94.
11. Wu Q, Zhang R. Weighted sum power maximization for intelligent reflecting surface aided SWIPT. IEEE Wireless Communications Letters. 2019;9(5):586-90.
12. Tang Y, Ma G, Xie H, Xu J, Han X, editors. Joint Transmit and Reflective Beamforming Design for IRS-Assisted Multiuser MISO SWIPT Systems. ICC 2020 - 2020 IEEE International Conference on Communications (ICC); 2020.
13. Khalili A, Zargari S, Wu Q, Ng DW, Zhang R. Multi-objective resource allocation for IRS-aided SWIPT. IEEE Wireless Communications Letters. 2021;10(6):1324-8.
14. Zargari S, Khalili A, Wu Q, Mili MR, Ng DW. Max-min fair energy-efficient beamforming design for intelligent reflecting surface-aided SWIPT systems with non-linear energy harvesting model. IEEE Transactions on Vehicular Technology. 2021;70(6):5848-64.
15. Liu J, Xiong K, Lu Y, Ng DW, Zhong Z, Han Z. Energy efficiency in secure IRS-aided SWIPT. IEEE Wireless Communications Letters. 2020;9(11):1884-8.
16. Sun W, Song Q, Guo L, Zhao J, editors. Secrecy Rate Maximization for Intelligent Reflecting Surface Aided SWIPT Systems. 2020 IEEE/CIC International Conference on Communications in China (ICCC); 2020.
17. Zargari S, Farahmand S, Abolhassani B. Joint design of transmit beamforming, IRS platform, and power splitting SWIPT receivers for downlink cellular multiuser MISO. Physical Communication. 2021;48:101413.
18. Tuan PV, Son PN. Intelligent reflecting surface assisted transceiver design optimization in non-linear SWIPT network with heterogeneous users. Wireless Networks. 2022;28(5):1889-908.
19. Kudathanthirige D, Gunasinghe D, Amarasuriya G, editors. Max-min Fairness-based IRS-aided SWIPT. GLOBECOM 2020 - 2020 IEEE Global Communications Conference; 2020.
20. Wu Q, Zhou X, Chen W, Li J, Zhang X. IRS-aided WPCNs: A new optimization framework for dynamic IRS beamforming. IEEE Transactions on Wireless Communications. 2021;21(7):4725-39.
21. Zargari S, Hakimi A, Tellambura C, Herath S. User Scheduling and Trajectory Optimization for Energy-Efficient IRS-UAV Networks With SWIPT. IEEE Transactions on Vehicular Technology. 2023;72(2):1815-30.
22. Boyd S, Boyd SP, Vandenberghe L. Convex optimization. Cambridge: Cambridge university press; 2004.
23. Grant M, Boyd S. CVX: Matlab software for disciplined convex programming, version 2.1; 2014.
24. Lobo MS, Vandenberghe L, Boyd S, Lebret H. Applications of second-order cone programming. Linear algebra and its applications. 1998;284(1-3):193-228.
25. Ben-Tal A, Nemirovski A. Lectures on modern convex optimization: analysis, algorithms, and

pISSN 1859-1388
eISSN 2615-9678

engineering applications. Philadelphia: Society for industrial and applied mathematics; 2001.

26. Karipidis E, Sidiropoulos ND, Luo ZQ. Quality of service and max-min fair transmit beamforming to multiple cochannel multicast groups. IEEE Transactions on Signal Processing. 2008;56(3):1268-79.

27. Goldsmith A, Wireless Communications. Cambridge: Cambridge university press; 2005.

28. Wu Q, Zhang R. Intelligent reflecting surface enhanced wireless network via joint active and passive beamforming. IEEE Transactions on Wireless Communications. 2019;18(11):5394-409.

29. Hu S, Wei Z, Cai Y, Liu C, Ng DW, Yuan J. Robust and secure sum-rate maximization for multiuser MISO downlink systems with self-sustainable IRS. IEEE Transactions on Communications. 2021;69(10):7032-49.

30. Priya TS, Mardeni R. Optimised COST-231 Hata models for WiMAX path loss prediction in suburban and open urban environments. Modern Applied Science. 2010;4(9):75-89.

31. Wu Q, Zhang R. Intelligent reflecting surface enhanced wireless network via joint active and passive beamforming. IEEE Transactions on Wireless Communications. 2019;18(11):5394-409.

32. Björnson E, Sanguinetti L. Power scaling laws and near-field behaviors of massive MIMO and intelligent reflecting surfaces. IEEE Open Journal of the Communications Society. 2020;1:1306-24.